J|A|C|S
ARTICLES
Published on Web 02/22/2006

In Situ Adsorption Studies of a 14-Amino Acid Leucine-Lysine Peptide onto Hydrophobic Polystyrene and Hydrophilic Silica Surfaces Using Quartz Crystal Microbalance, Atomic Force Microscopy, and Sum Frequency Generation Vibrational Spectroscopy

Ozzy Mermut,[†,‡] Diana C. Phillips,[†,‡] Roger L. York,[†,‡] Keith R. McCrea,[§] Robert S. Ward,[§] and Gabor A. Somorjai*[,†,‡]

Contribution from the Department of Chemistry, University of California, Berkeley, California 94720, Materials Science Division, Lawrence Berkeley National Laboratory, Berkeley, California 94720, and The Polymer Technology Group, 2810 Seventh Street, Berkeley, California 94710

Received September 1, 2005; E-mail: somorjai@socrates.berkeley.edu

Abstract: The adsorption of a 14-amino acid amphiphilic peptide, LK_{14}, which is composed of leucine (L, nonpolar) and lysine (K, charged), on hydrophobic polystyrene (PS) and hydrophilic silica (SiO_2) was investigated in situ by quartz crystal microbalance (QCM), atomic force microscopy (AFM), and sum frequency generation (SFG) vibrational spectroscopy. The LK_{14} peptide, adsorbed from a pH 7.4 phosphate-buffered saline (PBS) solution, displayed very different coverage, surface roughness and friction, topography, and surface-induced orientation when adsorbed onto PS versus SiO_2 surfaces. Real-time QCM adsorption data revealed that the peptide adsorbed onto hydrophobic PS through a fast ($t < 2$ min) process, while a much slower ($t > 30$ min) multistep adsorption and rearrangement occurred on the hydrophilic SiO_2. AFM measurements showed different surface morphologies and friction coefficients for LK_{14} adsorbed on the two surfaces. Surface-specific SFG spectra indicate very different ordering of the adsorbed peptide on hydrophobic PS as compared to hydrophilic SiO_2. At the LK_{14} solution/PS interface, CH resonances corresponding to the hydrophobic leucine side chains are evident. Conversely, only NH modes are observed at the peptide solution/SiO_2 interface, indicating a different average molecular orientation on this hydrophilic surface. The surface-dependent difference in the molecular-scale peptide interaction at the solution/hydrophobic solid versus solution/hydrophilic solid interfaces (measured by SFG) is manifested as significantly different macromolecular-level adsorption properties on the two surfaces (determined via AFM and QCM experiments).

Introduction

A fundamental understanding of the surface-induced adsorption behavior of biologically relevant peptides and their molecular conformation at polar and nonpolar interfaces is essential for the development of surface-modified biomaterials which are applicable to biofouling, biodiagnostics, proteomics, immunosensors, and tissue engineering.[1] The controlled immobilization of bioactive peptides onto various artificial bioplatforms (for example, via the hydrophobic effect) is the foundation for such technologies.[2−4] The behavior of synthetic short-chain amphiphilic peptides at solid interfaces is of particular interest, because they possess uniquely variable hydrophobic/hydrophilic domains. By controlling the amino acid sequence and relative content of these domains, one can promote specific interfacial interactions.[5,6] Achieving interface-directed orientation and conformational control of such peptides can be useful in the design of specific surface adaptors, in which selective functional sequences may be displayed for recognition or reception.[7,8]

As demonstrated by DeGrado and Lear, the distribution of hydrophobic and hydrophilic amino acid residues of a short peptide (<20 amino acids) can be tailored to match the repeat periodicity of a desired secondary structure which can be induced by the anisotropy of an nonpolar interface or by self-aggregation to form peptide micelles.[5,6,9] For example, lysine (K, charged) and leucine (L, nonpolar) amino acid residues sequenced with a hydrophobic periodicity of 3.6 and 2 residues/

[†] University of California.
[‡] Lawrence Berkeley National Laboratory.
[§] The Polymer Technology Group.

(1) Horbett, T. A.; Brash, J. L. *Proteins at Interfaces II: Fundamentals and Applications*; American Chemical Society: Washington, DC, 1995.
(2) Matsumura, M.; Fremont, D. H.; Peterson, P. A.; Wilson, I. A. *Science* **1992**, *257*, 5072.
(3) Russell, C. J.; Thorgeirsson, T. E.; Shin, Y. K. *Biochemistry* **1996**, *35*, 9526.
(4) Krüger, P.; Schalke, M.; Wang, Z.; Notter, R. H.; Dluhy, R. A.; Lösche, M. *Biophys. J.* **1999**, *77*, 903.
(5) DeGrado, W. F.; Lear, J. D. *J. Am. Chem. Soc.* **1985**, *107*, 7684.
(6) DeGrado, W. F.; Wasserman, Z. R.; Lear, J. D. *Science* **1989**, *243*, 622.
(7) Healy, K. E. *Curr. Opin. Solid State Mater. Sci.* **1999**, *4*, 381.
(8) Tong, Y. W.; Shoichet, M. S. *J. Biomater. Sci., Polym. Ed.* **1998**, *9*, 713.
(9) Kaiser, E. T.; Kezdy, F. J. *Proc. Natl. Acad. Sci. U.S.A.* **1983**, *80*, 1137.

10.1021/ja056031h CCC: $33.50

turn tend toward α-helical and *β*-sheet conformations, respectively, at the air/water interface. This occurs from maximizing the interactions of hydrophobic residues with a nonpolar interface. Thus, the residue composition (i.e., leucine/lysine molar ratio), charge periodicity, and nominal chain length serve as fundamental variables for directing peptide assembly into a desired amphiphilic secondary structure.[5,10−12] Previous studies of short-chain amphiphilic peptides have revealed that significant structural transitions can occur at an air/water interface (i.e., α-helix to random coil to *β*-sheet), which are highly time- and concentration-dependent.[13,14] The structural behavior is further complicated by accompanying changes in the aggregation state and solubility of the peptide.

The conformational behavior of amphiphilic peptides in solution and at the air/water interface has previously been studied; however, there is little experimental data available on peptide adsorption at solid surfaces.[5,13,15−18] This is attributed to the limited number of surface-specific techniques available for conformational analysis, which explicitly provide the necessary molecular-scale information (i.e., solid-state nuclear magnetic resonance and surface-enhanced Raman spectroscopy).[19−21] Even fewer techniques are amenable to interrogating peptide behavior at the solid/liquid interface, a buried interface, which is most applicable to biological systems.[22] Recent research efforts have demonstrated that imaging microscopy techniques, such as atomic force microscopy (AFM), can be valuable for studying the relation between molecular conformations of polypeptides and the morphology of adsorbed films on hydrophilic and hydrophobic surfaces.[23] However, it is difficult to quantify the amount of polypeptide adsorbed at an interface via imaging methods. The quartz crystal microbalance-dissipation (QCM-D) instrument is a highly sensitive surface mass detector (i.e., nanogram range) that is also capable of viscoelastic characterization (via energy dissipation measurements) of bound masses. While this analytic mass and viscoelasticity sensor is amenable to studies at the biological solution/solid interface, it lacks molecular specificity as does AFM. Sum frequency generation (SFG) is a vibrational spectroscopy that has recently emerged as a powerful technique for extracting molecular-level information of biomolecules at interfaces, including protein and peptide adsorption at the solid/air interface,[24,25] air/water interface,[26] and more recently at the biologically relevant solid/liquid interface.[27−30] SFG is an intrinsically surface-specific, nonlinear optical process.[31] Under the dipole approximation, this second-order process is forbidden in media that possess inversion symmetry. Inversion symmetry is necessarily broken at surfaces and interfaces, but rarely broken in bulk media. Although SFG has been successful in examining relative spatial ordering of proteins at biointerfaces, identifying specific amino acid interactions with the surface has proven to be difficult due to the large number of surface-interacting residues.[28,29,32] Thus, many questions remain regarding the driving forces and mechanism of adsorption of specific peptide sequences, which are suitable for investigation with surface-specific techniques.

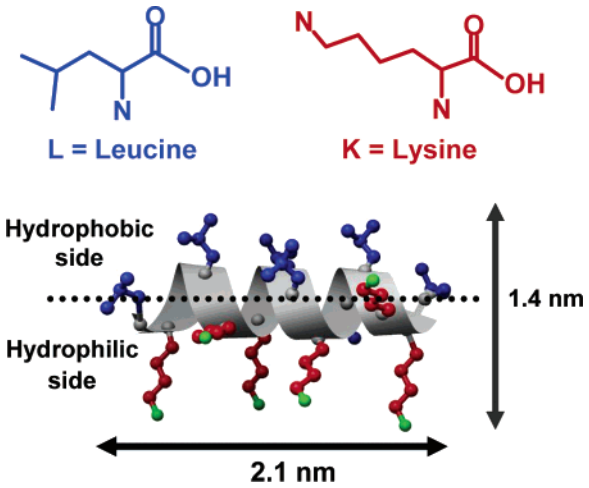

Figure 1. Ideal dimensions of the α-helical LK_{14} peptide in solution. Width across the helical barrel and total width including the side chains were calculated using ideal helical bond angles and van der Waals radii. The peptide forms tetramers under the solution conditions employed in the experiment.[5]

In the present work, we investigate the adsorption behavior of a model amphiphilic peptide, with sequence Ac(LKKLLKLL-KKLLKL)NH_2 (LK_{14}), on hydrophobic polystyrene (PS) and hydrophilic silica (SiO_2) surfaces using three in situ, surface-sensitive techniques. The peptide sequence was synthesized with a hydrophobic residue periodicity to favor induction of an α-helical configuration at a nonpolar surface or interface, allowing for investigation of the hydrophobic versus electrostatic bonding interactions upon adsorption. The formation of an α-helix in solution by this amphiphilic peptide induces a separation of the leucine (hydrophobic) and lysine (hydrophilic) side chains, as illustrated in Figure 1.[5]

Adsorption measurements using the QCM-D technique provided information regarding the peptide adsorption affinity for the hydrophobic versus hydrophilic surface as well as a direct comparison of the time scale for adsorption of the peptide film. This was achieved by monitoring frequency and energy dissipation changes which are related to the wet adsorbed mass and the elastic/viscoelastic nature of the adsorbed film, respectively. AFM was used to image the time-dependent morphology

(10) Brack, A.; Spach, G. *J. Am. Chem. Soc.* **1981**, *103*, 6319.
(11) Castano, S.; Desbat, B.; Dufourcq, J. *Biochim. Biophys. Acta* **2000**, *1463*, 65.
(12) Castano, S.; Desbat, B.; Cornut, I.; Méléard, P.; Dufourcq, J. *Lett. Pept. Sci.* **1997**, *4*, 195.
(13) Kerth, A.; Erbe, A.; Dathe, M.; Blume, A. *Biophys. J.* **2004**, *86*, 3750.
(14) Maget-Dana, R.; Lelievre, D.; Brack, A. *Biopolymers* **1999**, *49*, 415.
(15) Castano, S.; Desbat, B.; Laguerre, M.; Dufourcq, J. *Biochim. Biophys. Acta.* **1999**, *1416*, 176.
(16) Dieudonné, D.; Gericke, A.; Flach, C. R.; Jiang, X.; Farid, R. S.; Mendelsohn, R. *J. Am. Chem. Soc.* **1998**, *120*, 792.
(17) Blondelle, S. E.; Houghten, R. A. *Biochemistry* **1992**, *31*, 12688.
(18) Béven, L.; Castano, S.; Dufourcq, J.; Wieslander, Å.; Wroblewski, H. *Eur. J. Biochem.* **2003**, *270*, 2207.
(19) Long, J. R.; Oyler, N.; Drobny, G. P.; Stayton, P. S. *J. Am. Chem. Soc.* **2002**, *124*, 6297.
(20) Stewart, S.; Fredericks, P. M. *Spectrochim. Acta, Part A* **1999**, *55*, 1615.
(21) Herne, T. M.; Ahern, A. M.; Garrell, R. L. *Anal. Chim. Acta* **1991**, *246*, 75.
(22) Burkett, S. L.; Read, M. J. *Langmuir* **2001**, *17*, 5059.
(23) Lee, N. H.; Christensen, L. M.; Frank, C. W. *Langmuir* **2003**, *19*, 3525.
(24) Knoeson, A.; Pakalnis, S.; Wang, M.; Wise, W.; Lee, N.; Frank, C. W. *IEEE J. Sel. Top. Quantum Electron.* **2004**, *10*, 1154.
(25) Dreesen, L.; Sartenaer, Y.; Humbert, C.; Mani, A. A.; Méthivier, C.; Pradier, C. M.; Thiry, P. A.; Peremans, A. *Chem. Phys. Chem.* **2004**, *5*, 1719.
(26) Kim, G.; Gurau, M. C.; Lim, S. M.; Cremer, P. S. *J. Phys. Chem. B* **2003**, *107*, 1403.
(27) Chen, X.; Wang, J.; Sniadecki, J. J.; Even, M. A.; Chen, Z. *Langmuir* **2005**, *21*, 2662.
(28) Chen, X.; Clarke, M. L.; Wang, J.; Chen, Z. *Int. J. Mod. Phys. B* **2005**, *19*, 691 and references therein.
(29) Kim, J.; Cremer, P. S. *Chem. Phys. Chem.* **2001**, *2*, 543.
(30) Anderson, N. A.; Yang, C. S. C.; Stephenson, J. C.; Richter, L. J.; Briggman, K. A. *Abstr. Pap. Am. Chem. Soc.* **2005**, *229*, U669−U669.
(31) Raschke, M. B.; Shen, Y. R. *Curr. Opin. Solid State Mater. Sci.* **2004**, *8*, 343.
(32) Kim, J.; Somorjai, G. *J. Am. Chem. Soc.* **2003**, *125*, 3150.

of the adsorbed peptide film, as well as to compare the friction behavior exhibited by the adsorbed peptide on the two surfaces. SFG vibrational spectroscopy was employed to obtain surface-specific and molecular-level information regarding the interacting moieties and the relative ordering of surface-active amino acid residues at the solid/liquid (hydrophobic and hydrophilic) interface. By characterizing and contrasting the adsorbed morphology, friction, mass, dissipative energy, and average molecular orientation of the peptide on the two surfaces, we determined that the surface hydrophobicity dictates the surface interactions and adsorbed properties of the amphiphilic LK_{14}.

Experimental Section

LK_{14} Peptide Synthesis. LK_{14} peptide with sequence Ac(LKKLLKLL-KKLLKL)NH_2 was synthesized using an Advanced ChemTech (ACT) 396 automated synthesizer using standard 9-fluorenylmethyloxycarbonyl (FMOC) protocols.[33] Rink amide 4-methylbenzhydrylamine resin (Novabiochem) was prepared by swelling in 1-methyl-2-pyrrolidinone, then mixing with a FMOC-protected amino acid (Advanced ChemTech). The carboxylic acid group of the protected amino acid was activated prior to coupling to the resin by mixing with 1-hydroxybenzotriazole. The mixture was agitated (12 h) to ensure complete coupling of the first amino acid. The starter resin was then placed in the ACT instrument for completion of the synthesis. Acetylation of the N-terminus was accomplished by adding acetic anhydride to the resin-bound peptide. The peptide was cleaved from the resin in a solution of 95% trifluoroacetic acid and 5% water, precipitated from solution, and lyophilized to dryness. The peptide was purified using reversed-phase high-pressure liquid chromatography. The composition of the peptide was characterized, and electrospray ionization mass spectrometry (ESI-MS) showed M^{+2} and M^{+3} peaks corresponding to a mass of 1692.3 amu for the nonacetylated peptide. Lyophilized peptide samples were stored in a freezer (−15 °C), and a stock solution of 1 mM peptide in pH 7.4 phosphate-buffered saline (PBS; 0.01 M phosphate-buffered saline, 0.14 M NaCl, 0.0027 M KCl) solution was used for QCM, AFM, and SFG analysis. Ultrapure water (Millipore, Milli-Q 18 MΩ·cm) was used to prepare all solutions. For comparison across all techniques, all experiments were performed at low peptide concentration (0.1 mg/mL) unless otherwise stated. Peptides with this sequence (LK_{14}) have been shown to form tetrameric α-helical aggregates under the above solution conditions with hydrophobic leucine residues segregated to the core.[5]

Quartz Crystal Microbalance Measurements. Theoretical Background. As initially demonstrated by Sauerbrey, the QCM is a highly sensitive mass sensor capable of measuring nanogram quantities of adsorbed material on surfaces.[34] The mechanism involves exciting a piezoelectric crystal (through deposited metal electrodes) with an RF voltage near the crystal's resonant frequency and driving it to a shear oscillation.[34,35] After excitation, the voltage is switched off, and the decay in the voltage over the crystal is observed as an exponentially damped sinusoidal wave. The "wet" mass added (Δm) induces a linear resonant frequency shift (Δf) according to eq 1, provided that the adsorbed mass in a liquid environment is evenly distributed, and produces a sufficiently rigid and thin film (i.e., elastic masses are adsorbed). In eq 1, n denotes the overtone number and C is the mass sensitivity constant for $\Delta f = 1$ Hz (17.7 ng·cm^{-2} using a 5 MHz crystal).

$$\Delta m = -C\Delta f/n \quad (1)$$

In recent applications to biomolecular adsorption, the QCM technique has encountered much success attributed to both its highly sensitive detection of mass at the surface-solution interface and its capability to characterize the dissipative energy or viscoelastic behavior of the mass deposited.[35−38] In QCM-D, the variation in dissipation energy (ΔD) is measured concurrently with the frequency change and reflects the viscoelastic properties of the adlayer. The energy dissipation factor is defined as the ratio between the energy dissipated per oscillation cycle and the net stored energy in the oscillating system. For a perfectly elastic adsorbate, the change in energy dissipation is negligible. In systems where the adsorbate does not behave as an elastic mass (as in the case of many biomacromolecules),[39,40] significant dissipative losses occur due to internal and/or interfacial friction. This limits the validity of the Sauerbrey relation.[38]

Quartz Crystal Microbalance Measurements. Experimental Procedure. The wet mass of peptide adsorbed onto both the hydrophobic and hydrophilic surfaces was measured in the presence of PBS (pH = 7.4) using a QCM-D instrument (Q-Sense D300, Gothenburg, Sweden). SiO_2-coated sensor crystals (Q-Sense QSX 303, AT-cut, 5 MHz, active surface area = 0.2 cm^2) were employed as the hydrophilic supports. The substrates were exposed to a NOCHROMIX solution (24 h) and oxygen plasma treatment (2 min) prior to use. Hydrophobic supports were prepared by spin-coating a layer of 100-nm-thick PS (determined by AFM profiling) on SiO_2-coated sensors. The shift in resonance frequency (Δf) and dissipation (ΔD) was measured simultaneously at the fundamental ($n = 1$) and overtone ($n = 3, 5, 7$) frequencies. Prior to introducing the peptide solution to the sensor surface, the solution was thermally equilibrated in the T-loop of the QCM (0.5 mL at 25 ± 0.1 °C). The time allowed for thermal equilibration of the buffer within the crystal cell was determined by the period required to achieve a stable signal in the resonant frequency (5 and 25 min observed for the SiO_2 and the PS surfaces, respectively). The entire system was thoroughly cleaned with sodium dodecyl sulfate detergent (1 h) and flushed with water and ethanol (10 cycles) between sample measurements. Two replicate measurements were obtained for both the hydrophilic and hydrophobic surfaces.

Atomic Force Microscopy Measurements. Scanning probe images were obtained on a Molecular Imaging instrument using a 30-μm scan head (Pico SPM) in contact mode and at low loads (<5 nN). Prior to introducing peptide solutions, images of the bare SiO_2 and PS-coated SiO_2 surfaces were acquired in PBS (pH = 7.4). All AFM scanning was performed in situ using a gold-coated silicon nitride Si_3N_4 tip with a radius, $r = 15$ nm, and a nominal spring constant, $k = 0.2$ N·m^{-1} (Veeco Probes). The root-mean-square (rms) surface roughness was determined for a 2.5 μm × 2.5 μm surface. Friction data was also obtained at the peptide/buffer solution interface by laterally scanning a 200 nm × 200 nm area at 2 Hz (overtop the adsorbed peptide) at various normal force loads (0−17 nN). The normal loads applied were determined via calibration of the force−distance response curve on a silica substrate and converting into force using the spring constant of the tip. Friction experiments were performed at a peptide concentration of 1 mg/mL to ensure sufficient coverage of the surface and minimize convolution of substrate effects. A relative measure of the lateral force exhibited on the tip (measured in mV) at specified normal loads was determined from the average difference of the trace versus retrace image. The maximum load applicable to each surface was ascertained by the observation, upon rescanning, of load-induced permanent deformations to the surface. The relative friction was ascertained from the slope of the plot of lateral force (F_L) versus normal load (F_N).

Sum Frequency Generation Vibrational Spectroscopy. Theoretical Background. The theory of SFG has been described previously,

(33) King, D.; Fields, C.; Fields, G. *Int. J. Pept. Protein Res.* **1990**, *36*, 255.
(34) Sauerbrey, G. Z. *Phys.* **1959**, *155*, 206.
(35) Czanderna, A. W.; Lu, C. In *Applications of Piezoelectric Quartz Crystal Microbalances*; Lu, C., Czanderna, A. W., Eds.; Elsevier: Amsterdam, 1984; Vol. 7, p 1.
(36) Krim, J.; Chiarello, R. *J. Vac. Sci. Technol., B* **1991**, *9*, 1343.
(37) Widom, A.; Krim, J. *Phys. Rev. B* **1986**, *34*, 1403.
(38) Marx, K. A. *Biomacromolecules* **2003**, *4*, 1099.
(39) Höök, F.; Rodahl, M.; Brzezinski, P.; Kasemo, B. *Langmuir* **1998**, *14*, 729.
(40) Höök, F.; Kasemo, B.; Nylander, T.; Fant, C.; Sott, K.; Elwing, H. *Anal. Chem.* **2001**, *73*, 5796.

and an excellent introduction to the analysis of SFG spectra has been recently written.[41−43] In SFG spectroscopy, two pulsed laser beams, one of fixed frequency ω_{vis} (532 nm) and one of tunable frequency ω_{IR}, are overlapped spatially and temporally at an interface. Light at the sum frequency ω_{SFG} is collected in the reflected direction. The intensity of this light is proportional to the absolute square of the effective surface nonlinear susceptibility, $\chi_{eff}^{(2)}$:

$$I(\omega_{SFG}) \propto |\chi_{eff}^{(2)}|^2 I(\omega_{vis}) I(\omega_{IR}) \quad (2)$$

The effective surface nonlinear susceptibility is related to $\chi^{(2)}$, the surface nonlinear susceptibility through the tensorial Fresnel coefficients:[44]

$$\chi_{eff}^{(2)} = [\mathbf{L}(\omega_{SFG}) \cdot \mathbf{e}_{SFG}] \cdot \chi^{(2)} : [\mathbf{L}(\omega_{vis}) \cdot \mathbf{e}_{vis}][\mathbf{L}(\omega_{IR}) \cdot \mathbf{e}_{IR}] \quad (3)$$

where e_i is a unit polarization vector of the optical field at ω_i, and $\mathbf{L}(\omega_i)$ is the tensorial Fresnel factor.

The second-order nonlinear susceptibility has two components, a nonresonant term and, when the infrared beam is at a frequency that coincides with a frequency of a molecular vibration, a resonant term. This is expressed (in the dipole approximation) via:[44]

$$\chi^{(2)} = \chi_{NR}^{(2)} + N_S \langle \alpha_R^{(2)} \rangle_f = \chi_{NR}^{(2)} + N_S \int \alpha_R^{(2)} f(\Omega)\, d\Omega \quad (4)$$

where $\chi_{NR}^{(2)}$ comes from nonresonant excitations, N_S is the surface density of molecules, the symbol $\langle\ \rangle_f$ represents an orientational average over an orientation distribution function $f(\Omega)$, $\alpha_R^{(2)}$ is the resonant nonlinear hyperpolarizability (a tensor of rank 3), and Ω denotes a set of orientational angles that describes a transformation between the laboratory and molecular coordinate system.[44−46] The resonant nonlinear hyperpolarizability is composed of Lorentzian resonant terms:

$$\alpha_R^{(2)}(\omega_{IR}) = \sum_q \frac{\mathbf{a}_q}{\omega_{IR} - \omega_q + i\Gamma_q} \quad (5)$$

where $\mathbf{a}_q$ is the amplitude of the qth resonance, Γ_q is the line width (or damping factor) of the qth resonance, ω_{IR} is the IR frequency, and ω_q is the frequency of the qth molecular vibration. As the IR frequency is scanned across the IR, ω_{IR} comes into resonance with ω_q, the resonant term, and SFG signal intensity is enhanced. The amplitude of the qth resonance term, $\mathbf{a}_q$, is understood from sum frequency theory as:

$$\mathbf{a}_q \propto \frac{\partial \vec{\boldsymbol{\mu}}}{\partial Q_q} \otimes \frac{\partial \boldsymbol{\alpha}^{(1)}}{\partial Q_q} \quad (6)$$

where $\partial\vec{\boldsymbol{\mu}}/\partial Q_q$ and $\partial\boldsymbol{\alpha}^{(1)}/\partial Q_q$ are the infrared dipole derivative and Raman polarizability derivative with respect to Q_q, the classical normal coordinate of the qth vibrational mode, respectively.[44,47] According to eqs 2−6, a vibrational resonance is SFG-active when it is both IR-active and Raman-active.[48,49] The integral in eq 4 demonstrates how the orientation distribution of a molecule can change its SF spectra. For an adsorbate with many IR- and Raman-active modes, the way in which the adsorbate bonds with the interface can change the orientation distribution and hence the intensity of the modes that appear in the SFG spectra. This is because at a given interface, some parts of the molecule may have different geometrical orientations due to specific interactions with the surface.[50,51] As a result, specific surface interactions can cause some modes to produce SFG signal at certain interfaces, while other modes may be SFG-active at different interfaces.

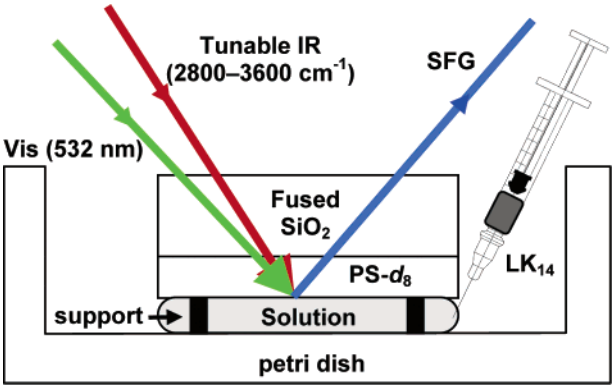

Figure 2. Schematic of the SFG experimental setup. The hydrophobic PS-d_8/aqueous PBS interface is created by spin-coating PS-d_8 (300 nm) onto SiO_2 windows and exposing it first to PBS solution, followed by injection of the LK_{14} solution. The hydrophilic SiO_2/aqueous interface is similarly prepared by direct exposure to the solution (no PS-d_8 spin-coated).

Sum Frequency Generation Vibrational Spectroscopy. Laser System and Data Collection. SFG spectra were obtained with a mode-locked Nd:YAG laser (Ekspla, Lithuania). The 1064-nm light generated has a pulse width of 20 ps, and the laser operates at a 10 Hz repetition rate. Radiation is sent to an optical parametric generator/amplifier (OPG/OPA) stage (LaserVision, Bellevue, WA) where tunable infrared radiation is produced in addition to frequency-doubled radiation at 532 nm. The OPG/OPA consists of two parts. The first is an angle-tuned potassium titanyl phosphate (KTP) stage pumped with 532-nm light to generate near-infrared radiation between 1.35 and 1.85 μm. This output is then mixed with the 1064-nm fundamental in an angle-tunable potassium titanyl arsenate (KTA) stage to produce a tunable infrared beam from 2000 to 4000 cm^{-1} (7 cm^{-1} fwhm). As shown schematically in Figure 2, the tunable infrared beam is combined with the 532-nm radiation at the sample interface at incident angles of ca. 62° and 58°, respectively, with respect to the surface normal.

The SFG signal generated from the sample is collected by a photomultiplier tube, sent to a gated integrator, and stored digitally. For each scan, data is collected with 10 shots/data point in 5 cm^{-1} increments in the 2800−3600 cm^{-1} range. For a given condition, SFG measurements were repeated at least six times to increase the signal-to-noise ratio, and the collected data were averaged to produce the final spectra presented in this article. All spectra shown were collected with the *ssp* (sum, visible, infrared, respectively) polarization combination.

Sample Preparation. Fused silica windows (Esco Products) were cleaned by soaking in a saturated NOCHROMIX (Godax Laboratories) oxidizing solution and rinsing with deionized water. Polystyrene thin films (200 nm) were prepared by spin-casting (Specialty Coating Systems, P-6000 spin coater) a 3 wt % solution of deuterated polystyrene (PS-d_8, MW ≈ 300 000, Polymer Source, Inc.) in toluene onto the fused silica windows and annealing at 110 °C (12 h). Background QCM, AFM, and SFG measurements were obtained on clean PS and SiO_2 surfaces in PBS solution prior to addition of the peptide solution. Contact with air was minimized by introducing the peptide solution directly to the buffer/solid interface (Figure 2). For example, the solid substrate placed on top of a reservoir of peptide solution exposed to the air/water interface produced different SFG

(41) Lambert, A. G.; Davies, P. B.; Neivandt, D. J. *Appl. Spectrosc. Rev.* **2005**, *40*, 103.
(42) Shen, Y. R. *Nature* **1989**, *337*, 519.
(43) Wang, H. F.; Gan, W.; Lu, R.; Rao, Y.; Wu, B. H. *Int. Rev. Phys. Chem.* **2005**, *24*, 191.
(44) Wei, X.; Hong, S. C.; Zhuang, X.; Goto, T.; Shen, Y. R. *Phys. Rev. E* **2000**, *62*, 5160.
(45) Hirose, C.; Akamatsu, N.; Domen, K. *Appl. Spectrosc.* **1992**, *46*, 1051.
(46) Zhuang, X.; Miranda, P. B.; Kim, D.; Shen, Y. R. *Phys. Rev. B* **1999**, *59*, 12632.
(47) Superfine, R.; Huang, J. Y.; Shen, Y. R. *Chem. Phys. Lett.* **1990**, *172*, 303.
(48) Doyle, A. W.; Fick, J.; Himmelhaus, M.; Eck, W.; Graziani, I.; Prudovsky, I.; Grunze, M.; Maciag, T.; Neivandt, D. J. *Langmuir* **2004**, *20*, 8961.
(49) Wang, J.; Buck, S.; Chen, Z. *J. Phys. Chem. B* **2002**, *106*, 11666.
(50) Baldelli, S.; Mailhot, G.; Ross, P. N.; Somorjai, G. A. *J. Am. Chem. Soc.* **2001**, *123*, 7697.
(51) Baldelli, S.; Mailhot, G.; Ross, P.; Shen, Y. R.; Somorjai, G. *J. Phys. Chem. B* **2001**, *105*, 654.

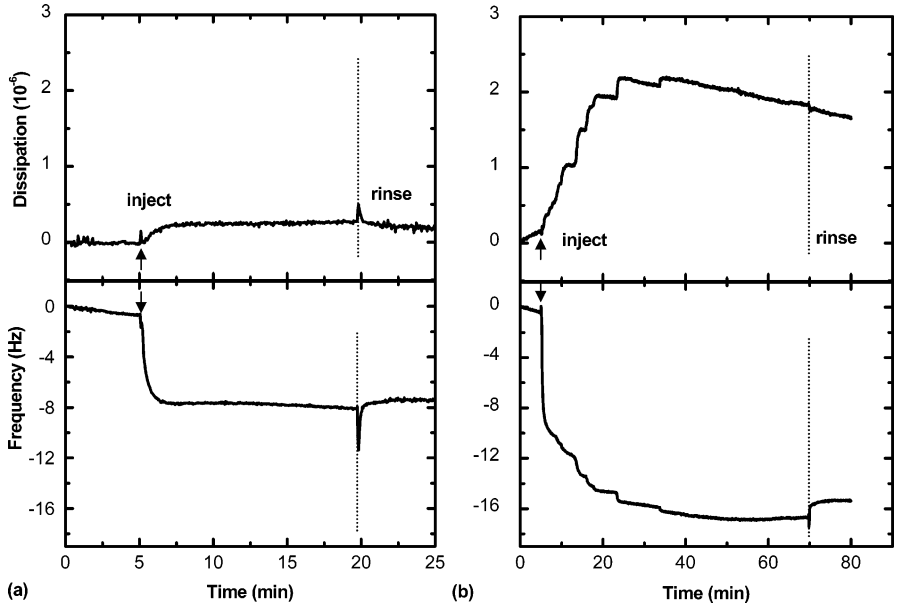

Figure 3. Real-time change in energy dissipation (top) and frequency (bottom) resulting from LK_{14} adsorption onto (a) PS and (b) SiO_2. On PS, a typical single-step exponential adsorption is observed in <2 min, while on SiO_2 a multistep process occurs over 35 min.

spectra (similar to dried peptide film spectra), possibly indicating the formation of a Langmuir−Blodgett peptide film at the air/water interface.

Results

(a) Quartz Crystal Microbalance Measurements of LK_{14} Adsorption onto PS versus SiO_2. Using a QCM-D, we monitored the adsorption process of the LK_{14} peptide (0.1 mg/mL) in situ on both hydrophobic and hydrophilic surfaces. Figure 3a,b shows the change in frequency and dissipation (at $n = 3$ overtone) as the peptide is adsorbed onto the PS and SiO_2 surfaces, respectively. The arrows mark the starting point of the measurement when the peptide solution is exposed to the surface ($t = 0 = \Delta f = \Delta D$). The vertical dashed lines indicate the end of the experiment when the surface is flushed with buffer solution. The spikes in frequency and dissipation upon peptide injection and rinsing with buffer are due to transient variations in pressure and temperature as new solutions are introduced.

On PS, the peptide displays the simple exponential adsorption behavior characteristic of single-step adsorption described by first-order kinetics.[52] AFM results, presented later, show partial surface coverage of the adsorbed monolayer. The adsorption occurs in ~2 min with a shift in frequency and dissipation of $\Delta f = -7.4$ Hz and $\Delta D = 0.26 \times 10^{-6}$, respectively. Upon washing the LK_{14}/PS surface with buffer at $t = 20$ min, only minor desorption, corresponding to less than 0.5 Hz in frequency shift, was observed.

A markedly different multistep (nonmonotonic) behavior is observed in both Δf and ΔD when LK_{14} adsorbs on SiO_2. The total frequency shift of −15.4 Hz is accompanied by a significant increase in the total dissipation, $\Delta D = 1.5-2.0$ ($\times 10^{-6}$). Unlike the hydrophobic surface, washing LK_{14}/SiO_2 with PBS induced a positive frequency shift of 1.6 Hz ($t = 70$ min). A large drop in frequency ($\Delta f_1 = -9$ Hz) is initially observed up to $t = 5$ min, subsequently followed by smaller, nonequivalent steps ($\Delta f_{2,3,4} \approx -1$ Hz) up to $t = 35$ min.

(52) Keller, C. A.; Kasemo, B. *Biophys. J.* **1998**, *75*, 1397.

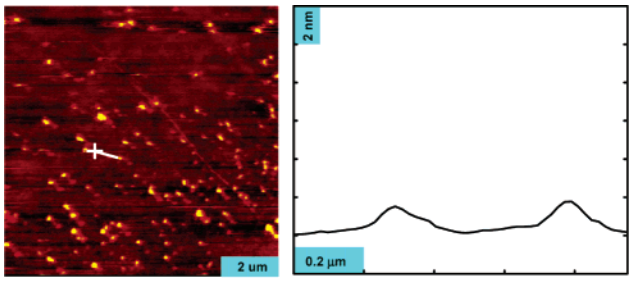

Figure 4. AFM of 0.1 mg/mL LK_{14} adsorbed onto PS showing 1.5-nm heights imaged after 5 min. Similar topographic heights are observed at longer time scales.

(b) Atomic Force Microscopy Measurements of LK_{14} Adsorption onto PS versus SiO_2. AFM images of the adsorbed peptide on the hydrophobic and hydrophilic surfaces were obtained in situ at two concentrations (1 and 0.1 mg/mL). The adsorbed morphology of LK_{14} on the polystyrene surface at low concentration of peptide is displayed in Figure 4.

AFM analysis of LK_{14} adsorbed on polystyrene at higher concentrations is not presented due to the absence of observable features, presumably from increased coverage resulting in a smooth monolayer. Adsorption at low concentration induced an increase in rms roughness from 0.4 ± 0.1 nm (featureless bare PS) to 0.8 ± 0.2 nm (LK_{14}/PS, round features ~200 nm wide). The AFM cross section profile shows topographical features as small as 1.5 nm in height.

Figure 5a shows the morphology of low-concentration LK_{14} adsorbed onto SiO_2 at $t < 5$ min. In comparison to the bare silica surface (rms surface roughness of 0.2 ± 0.1 nm), adsorption of the peptide induced a 4-fold increase in the roughness to 0.7 ± 0.1 nm within minutes of exposure to SiO_2. Initially, the peptide exhibits a spherically aggregated morphology. The lateral dimensions are between 150 and 300 nm and appear monodisperse (although polydispersity was not explicitly measured). Unlike the PS surface, we measured feature heights of distinctly 2.5 or 5.0 nm. Between 5 and 10 min of adsorption, we observed significant lateral aggregation and an increase in the density of surface features, as evidenced by the 7-fold rise

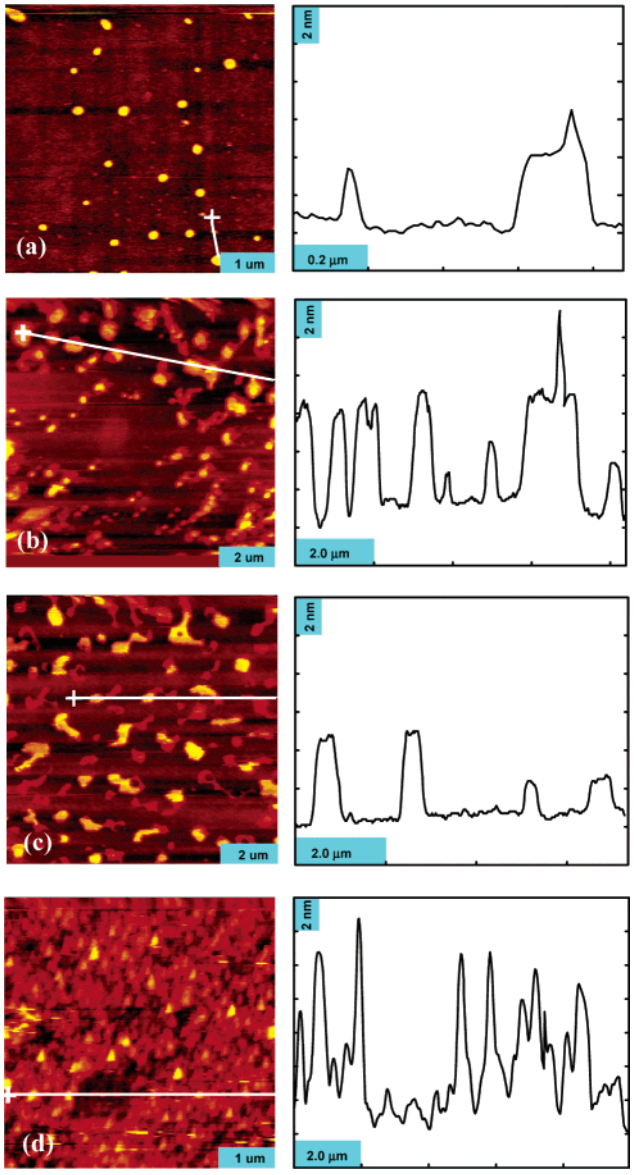

Figure 5. AFM topographical features from 0.1 mg/mL LK_{14} adsorbed onto SiO_2 (showing distinctly 2.5- and 5.0-nm heights) imaged at: (a) <5 min, (b) 5−10 min, (c) >30 min. Image of LK_{14} adsorbed at a higher solution concentration (l mg/mL) is displayed in (d). The depressed region on the film (dark square) is the result of scanning at a normal force >17 nN and inducing damage to the film.

in roughness to 1.2 ± 0.3 nm (Figure 5b). At $t = 5-10$ min, the surface-bound LK_{14} displays larger lateral size distribution with features ranging from 0.2 to 1.0 μm in width. However, this lateral expansion is not accompanied by an incremental growth in feature height, as revealed in Figure 5b (i.e., topographic heights of 2.5 nm and predominantly 5.0 nm remain constant). An image obtained after 30 min of adsorption yields a surface roughness of 1.3 ± 0.1 nm (Figure 5c). Topographical analysis reveals that the LK_{14} undergoes a gradual morphological transition on SiO_2 from small, spherical islands (~200-nm wide) to much larger, laterally aggregated domains (up to 1.5 μm) over a 30-min period.

Using a 10-fold higher concentration of peptide (1 mg/mL) produces a very different topography on SiO_2, as shown in Figure 5d. In this case, we immediately observe a large quantity of densely packed LK_{14}, displaying feature heights of >10 nm. The massive deposition of peptide is also accompanied by a 12-fold increase in the roughness from 0.18 ± 0.1 to 2.3 ± 0.2 nm. At high concentrations, no time-dependent perturbation of the height or feature width is seen via AFM.

Using AFM lateral force detection, we also obtained the friction force exhibited by the adsorbed LK_{14} (1 mg/mL) on both the hydrophobic and hydrophilic surfaces (Figure 6). Note that the maximum normal load capacity on the LK_{14}/PS and LK_{14}/SiO_2 systems was 2 and 17 nN, respectively. In the case of LK_{14} adsorbed onto SiO_2, the surface friction doubled compared to that of the bare surface, as indicated by the slopes of the lateral force plots. Conversely, the LK_{14} adsorption onto PS did not produce a significant change in the friction force and slightly decreased by a factor of 1:0.8 (bare PS:LK_{14} on PS).

(c) SFG Data of LK_{14} Adsorbed onto PS-d_8 versus SiO_2. We conducted SFG experiments on deuterated polystyrene (PS-d_8) and SiO_2 before and after adsorption of a 0.1 mg/mL LK_{14} peptide solution to examine the effect of the interface hydrophobicity on the surface interaction of the adsorbate. These substrates are suitable for the SFG study because neither generate SFG features in the spectral region under study (2800−3600 cm^{-1}). The SFG spectra of amphiphilic LK_{14} adsorbed to a hydrophobic (Figure 7) and hydrophilic (Figure 8) surfaces indicate that the nature of the adsorption is strongly dependent on the surface hydrophobicity.

The solid lines in Figures 7 and 8 are the least-square fits of the raw SFG data to eq 5, and the observed peaks are summarized in Table 1. Background SFG spectra of PBS on the bare surfaces are plotted in the lower traces of Figures 7 and 8. On the hydrophobic PS-d_8, only OH stretching modes (3092 cm^{-1}) (before and after peptide adsorption) are assigned to structured water molecules. Upon peptide adsorption, the CH stretching modes observed in the SFG spectrum of LK_{14} adsorbed on PS-d_8 are assigned to CH_3 symmetric (2869 cm^{-1}) Fermi resonance of methyl symmetric stretch (2935 cm^{-1}).[53] The mode at 2895 cm^{-1} is assigned to either CH or a methylene Fermi resonance, in agreement with previous studies of the leucine amino acid.[53,54]

On the hydrophilic SiO_2/water interface, we observe peaks from OH modes at ~3200 and ~3400 cm^{-1} from the hydrogen-bonded water. Upon injecting LK_{14} into the PBS solution, we find that the OH modes decrease in intensity and a NH stretching mode appears (Figure 8). As later discussed, the assignment of the NH mode is not trivial since the LK_{14} peptide contains NH_3^+ moieties on the lysine side chains and the N-terminus of the peptide backbone, as well as NH moieties in the peptide backbone (designated Amide A). The amplitude of the small peak observed around 2870 cm^{-1} is on the order of the noise and is therefore not fit. The differences in the peak intensities of the CH and NH modes are due to differences in the various contributions to the SFG signal (i.e., Raman polarizability, IR dipole transition amplitude, number of oscillators/surface concentration, and average molecular orientation).

Discussion

(a) Quartz Crystal Microbalance Studies of Amphiphilic LK_{14} Adsorption on Hydrophobic and Hydrophilic Surfaces. On PS, the net $\Delta f = -7.4$ Hz corresponds to LK_{14} adsorption

(53) Ji, N.; Shen, Y. R. *J. Chem. Phys.* **2004**, *120*, 7107.
(54) Watry, M. R.; Richmond, G. L. *J. Phys. Chem. B* **2002**, *106*, 12517.

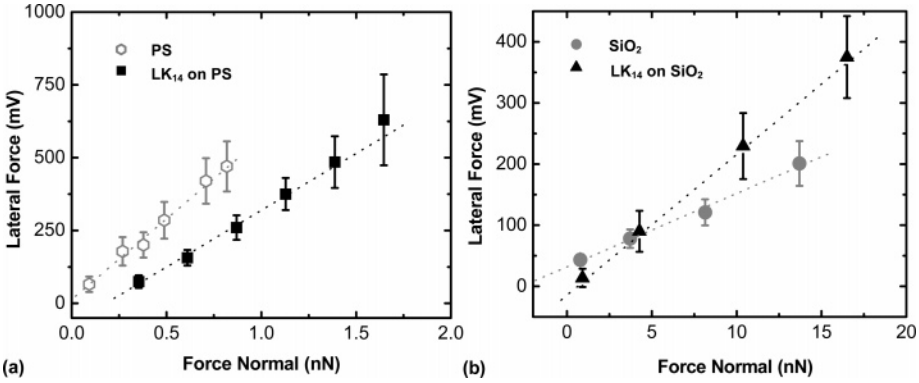

Figure 6. Relative friction behavior (obtained by the slope of F_L/F_N) of LK_{14} (1 mg/mL) adsorbed onto (a) PS and (b) SiO_2. A small decrease in friction occurs upon LK_{14} adsorption onto PS as indicated by the ratio of the slopes of the bare surface to LK_{14}/PS (1:0.8). Friction is doubled after LK_{14} adsorption on SiO_2.

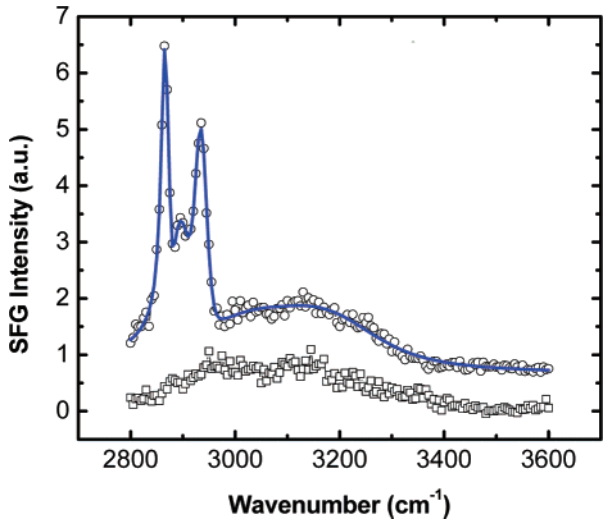

Figure 7. SFG spectrum of PBS solution (lower trace) and LK_{14} (upper trace) adsorbed onto PS-d_8. The broad peak centered at 3092 cm^{-1} is assigned to structured water molecules. Peaks at 2869 cm^{-1} (CH_3 symmetric), 2895 cm^{-1} (CH or CH_2 Fermi resonance), and 2935 cm^{-1} (CH_3 Fermi resonance) are observed.

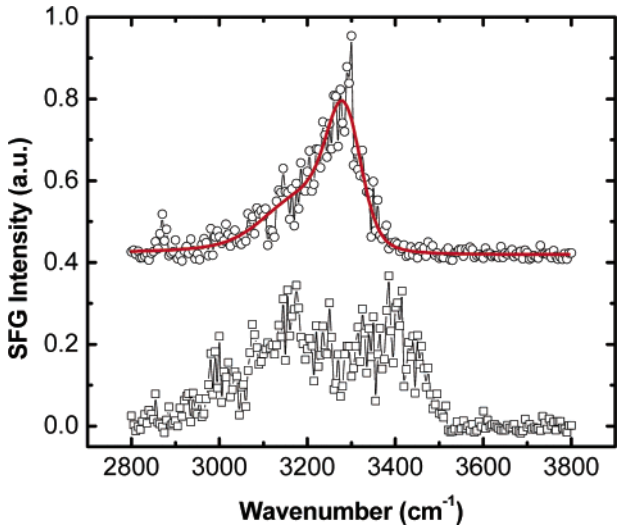

Figure 8. SFG spectrum of PBS solution (lower trace) and LK_{14} (upper trace) adsorbed onto SiO_2. The dominant peak at 3294 cm^{-1} is assigned to an NH stretching mode, and a weak OH peak is observed at ~3190 cm^{-1}.

Table 1. SFG Peak Assignments for LK_{14} Adsorbed on PS-d_8 and SiO_2

surface	frequency (cm^{-1})	mode
PS-d_8	2869	$CH_{3\,vs}$
PS-d_8	2895	CH or FR_{CH2}[a]
PS-d_8	2935	FR_{CH3}[b]
PS-d_8	3092	OH
SiO_2	3190	OH
SiO_2	3294	NH

[a] Methylene Fermi resonance. [b] Methyl Fermi resonance.

with hydrated mass of 130 ng·cm^{-2}. The monolayer of the peptide is stable, exhibiting negligible desorption upon washing the LK_{14}/PS surface with buffer ($\Delta f_{wash} \approx 0$). The adsorption occurs in a single-step process, reaching steady state within ~2 min. The accompanying low-energy dissipation shift ($\Delta D = 0.26 \times 10^{-6}$) suggests the formation of a more rigidly adsorbed film predominating on the hydrophobic surface. This justifies the Sauerbrey-derived quantification of the adsorbed mass on PS.

The adsorption of LK_{14} onto SiO_2 produces a very different multistep pattern in the QCM-D measurements (both in Δf and in ΔD), suggesting a stepwise growth of the peptide film on the hydrophilic surface. Similar multistep adsorption behavior has previously been observed in QCM studies of charged biomolecules in multilayer assemblies.[55] One must keep in mind that the response in Δf and ΔD reflects the average adsorption across the active surface area of the crystal and does not necessarily imply saturated coverage of the surface. Thus, the stepwise adsorption observed can correspond to either formation of unique layers of LK_{14} and/or increasing fractional coverage of the surface. To determine this, one needs knowledge of the 3D conformation and footprint of the adsorbed LK_{14}.[52] However, the AFM data show a time-dependent adsorption of laterally irregular islands with constant heights of 2.5 and 5 nm, suggesting the formation of some layers. In light of the AFM data, the stepwise reduction in frequency observed by QCM likely represents a multistep (and multilayer) adsorption process of LK_{14} on SiO_2. The time-dependent AFM results suggest that the beginning step involves the rapid adsorption to form several nucleation sites on the surface (i.e., several LK_{14} molecules adsorbed overtop one another). Slower adsorption processes subsequently follow, including island growth and spreading over the SiO_2, leading to larger laterally coalesced domains.

(55) Calvo, E. J.; Danilowicz, C.; Lagier, C. M.; Manrique, J.; Otero, M. *Biosens. Bioelectron.* **2004**, *19*, 1219.

Evidence for a multistep process that involves different types of surface interactions occurring on SiO_2 (i.e., peptide/surface and peptide/peptide interactions) is given by the nonequivalence of the adsorption steps (Figure 3). Specifically, the frequency change associated with the initial adsorption step ($\Delta f_1 = -9$ Hz) is dissimilar to subsequent adsorption processes ($\Delta f_{2,3,4} \approx -1$ Hz) with respect to the adsorbed amount and time of each step. This outcome suggests that several adsorption mechanisms contribute. The later stages of adsorption ($t = 10-40$ min) involve much weaker interactions (i.e., peptide/peptide) than the initial LK_{14}/SiO_2 surface interaction. Furthermore, ~10% of total adsorbed mass can be removed by washing as evidenced by the increase in Δf_{wash} by 1.6 Hz. This confirms the presence of weaker interactions within the uppermost peptide layers.

A significant change in dissipation is also noted with peptide adsorption onto SiO_2, $\Delta D = 1.5-2.0$ ($\times 10^{-6}$). This is markedly different from the small dissipation response of $\Delta D = 0.26 \times 10^{-6}$ accompanying adsorption onto PS. The difference in dissipation behavior further supports the idea that the peptide adsorbs very differently on the two surfaces. Although the total decrease in frequency on SiO_2 ($\Delta f_1 = -15.4$ Hz) is approximately twice that on PS ($\Delta f = -7.4$ Hz), the large net change in dissipation on the hydrophilic SiO_2 implies significant viscoelastic behavior of nonrigid LK_{14} adlayers. Thus, the Sauerbrey relation is not valid on the hydrophilic surface, and quantitative analysis of the steps (i.e., conversion of the *f* shift to a hydrated peptide mass) is nontrivial.[39] Furthermore, at the onset of each adsorption step, a gradual decrease in ΔD is followed. This result implies that adsorbed LK_{14} molecules on SiO_2 are more dynamic than those on PS. Initially, adsorbed LK_{14} on SiO_2 is highly mobile (exhibiting high viscous losses) and undergoes observable rearrangements on the surface. As adsorption continues within a step, a reduced ΔD indicates a decrease in the mobility of peptide molecules over time.

The effect of the surface hydrophobicity is also expressed in the different adsorption kinetic time scales observed. For instance, LK_{14} exhibits rapid initial adsorption on both surfaces (on the order of seconds) as indicated by the initial large decrease in the frequency in both cases ($\Delta f_1 = -9$ Hz for SiO_2 and $\Delta f = -7.4$ Hz for PS). However, the adsorption reaches equilibrium in ~2 min on hydrophobic PS surface, while on hydrophilic SiO_2 the multistep mechanism requires ~35 min.

(b) AFM Studies of Amphiphilic LK_{14} Adsorption on Hydrophobic and Hydrophilic Surfaces. Topographical analysis of LK_{14} (0.1 mg/mL) adsorbed onto the hydrophobic surface shows feature heights of 1.5 nm. Under similar solution conditions, circular dichroism studies indicate that the LK_{14} is α-helical.[5] While the precise secondary structure of the peptide on the surface has not been definitively identified here, this height is similar to the calculated (defect-free) van der Waals diameter of the LK_{14} α-helix in solution (1.4 nm = width of helical barrel plus the K and L side chains as shown in Figure 1). The tetrameric aggregation state is a consequence of the hydrophobic leucine residues segregating and self-associating to create a hydrophobic core, with the free energy of dehydration of the hydrophobic side chains being the driving force. Therefore, despite using a peptide and buffer salt concentration that stabilizes tetramer formation of LK_{14} in solution, the measured feature heights of 1.5 nm suggest that some peptides undergo an adsorption-induced reduction in aggregation state. When the amphiphilic peptide is adsorbed on a hydrophobic surface, the unfolding of the tetrameric aggregates is likely stabilized by the strong newly formed hydrophobic interactions resulting from adsorption onto PS. Such a hydrophobic driven adsorption would reduce the interfacial energy by exposing the hydrophobic residues of the interior tetramer to the hydrophobic surface. Similar observations have been reported in fluorescence and circular dichroism studies by Kiyota et al. which examined aggregated small-chain LK peptides interacting with a lipid bilayer, an analogous liquid/solid interface.[56] Here, the small-chain amphiphilic peptide undergoes gradual transition from a self-aggregated state in buffer solution to a single α-helix upon interaction with lipid bilayers.[56] This reduction in aggregation is primarily attributed to the hydrophobic-mediated interactions of hydrophobic residues with the interior of the lipid bilayer, with the absence of electrostatic interactions. Interestingly, no dynamic effects were detected on the time scale of the AFM measurements (5 min to 2 h) for LK_{14} feature dimensions on PS. For example, no time-dependent increase in the density of surface features or lateral growth/surface aggregation was resolved by AFM, indicating that immediate adsorption of peptide had occurred. This result agrees with the rapid adsorption ($t \approx 2$ min) observed by QCM on PS.

With adsorption occurring at the same concentration but onto a hydrophilic surface, a strong dynamic effect on both the adsorbed amount and the lateral growth of the peptide is observed by AFM. Over the 30-min adsorption process, a significant increase in the density of adsorbed peptide was evident by the transition of small spherical agglomerates (150−300 nm in width) to large laterally disperse islands (up to 1.5 μm in width). Furthermore, a time-dependent increase in the rms surface roughness from 0.2 ± 0.1 nm (bare silica) to 0.7 ± 0.1 nm (LK_{14} on SiO_2 at $t < 5$ min) and finally to 1.3 ± 0.1 nm (LK_{14} on SiO_2 at $t > 30$ min) confirms that gradual adsorption, over $t > 30$ min, occurs on a hydrophilic surface, which is much different than the $t < 2$ min time scale on the hydrophobic PS (rms roughness = 0.8 ± 0.2 nm). In light of the multistep behavior observed by QCM, the increase in adsorbed amount after the initial step likely includes gradual mass deposition via aggregation processes across the surface. While the lateral size distribution changes significantly throughout the LK_{14} deposition, the topographical heights remain discrete (2.5 and 5.0 nm) over time. Thus, the initial step likely involves the formation of discrete numbers of stacked LK_{14} molecules (i.e., nucleation sites), which may be similar in orientation and, hence, height. At higher concentrations, many layers of stacked LK_{14} molecules are formed on top of the SiO_2 as suggested by AFM measured heights of >10 nm. In this case, the lateral dimensions and geometry of the features observed in the uppermost layers of peptide appear to be homogeneous (around 150−200 nm) and similar to those of the exposed lower layers, as seen in Figure 5d. This suggests that, at higher concentrations of LK_{14}, the adsorption is influenced by peptide self-association in solution prior to interaction with the SiO_2 surface. This idea is consistent with previous research, which has shown that the use of higher concentrations of amphiphilic LK_{14} peptide in aqueous solution tends to promote self-aggregation.[5]

(56) Kiyota, T.; Lee, S.; Sugihara, G. *Biochemistry* **1996**, *35*, 13196.

The difference in the friction behavior obtained on the two LK_{14}-coated surfaces is rationalized by the variation in surface interactions occurring upon adsorption onto PS versus that on SiO_2. This is confirmed by results obtained from the SFG studies. As suggested by the AFM topographic data, different driving forces are likely responsible for the different adsorption states of LK_{14} on hydrophobic versus hydrophilic surfaces. A rough surface containing features of 5 nm (i.e., produced by LK_{14} on SiO_2) is expected to exhibit a larger lateral force on a dragging tip due to contact with a large number of surface asperities, as compared to a more smooth film containing a lower density of adsorbed LK_{14} and having smaller feature heights of 1.5 nm (i.e., exhibited by LK_{14} on PS). Thus, it is not surprising that larger normal forces up to 17 nN could be exerted onto the thick multilayers of the LK_{14}/SiO_2 system before inducing permanent deformation to the surface (shown in Figure 5d), while the damage threshold on LK_{14}/PS layer was significantly less at 2 nN.

(c) SFG Conformational Analysis of Adsorbed LK_{14} on Hydrophobic and Hydrophilic Surfaces. The presence of ordered methyl groups of the adsorbed leucine side chains on the PS-d_8 versus ordered NH on SiO_2 corroborates the AFM and QCM data, which indicate very different adsorption behavior on the two surfaces. The SFG data suggest that the preferential average orientation of the LK_{14} peptide on the surface is dictated by the nature of the favored interactions occurring at the solid/liquid interface. While these SFG studies in the CH region cannot confirm the precise structure on the surface (requiring SFG experiments in the spectral region between 1200 and 1800 cm^{-1}),[27,57] AFM and QCM data suggest the formation of a rigid 1.5-nm-thick monolayer on PS-d_8. The hydrophobic interaction of the leucine side chains with the PS-d_8 surface is likely driven by the dissociation of the solution-phase tetramers. This surface-mediated dehydration of the side chains would minimize the surface energy. Thus, it is thermodynamically reasonable that the surface-bonding of the peptide through the leucine residues on the hydrophobic surface allows interaction of the charged lysine residues with the aqueous bulk.

On silica, the observation of NH stretching modes (and the absence of CH stretching modes) indicates LK_{14} peptide bonds with different ordering (and hence different orientational distribution function) at this hydrophilic solid/water interface. The hydrophilic SiO_2 is a negatively charged surface in a pH $= 7.4$ solution ($pK_a = 2$), which suggests an electrostatic adsorption mechanism on this surface, proposed to occur through the positively charged lysine side chains ($pK_a = 10$). Furthermore, AFM shows that multiple peptide layers are formed on this hydrophilic surface, which can be driven from the intermolecular self-association of the leucine side chains to minimize the interfacial energy from contact with the bulk water. It is therefore feasible that the detected NH mode is from the side chains of the lysine residues and is in agreement with a recent SFG study assigning the mode to the positively charged side-chain amino acids of proteins adsorbed on silica.[58] However, the NH assignment to an Amide A mode cannot be ruled out, since Amide A is normally observed between 3270 and 3310 cm^{-1}.[59] Regardless of the exact origin of the observed signal, the difference in SFG spectra between the hydrophobic and hydrophilic surface indicates the peptide has *completely different average orientations at these interfaces*.

We also observe drastically different peaks in the water region on the hydrophilic versus hydrophobic surface. A large broad OH peak centered at 3092 cm^{-1} is always observed for LK_{14}/PS-d_8 (Figure 7) in comparison to a much weaker peak at 3190 cm^{-1} for LK_{14}/SiO_2 (Figure 8). Although the OH peak at 3092 cm^{-1} is a low frequency for water, SFG results of hydrophobic solid/water interfaces have shown broad OH modes that span the region between 3000 and 3600 cm^{-1} due to different hydrogen-bonded environments.[60] According to the literature, and in the absence of peptide, OH peaks typically observed at $\sim$3200 and $\sim$3400 cm^{-1} are attributed to tetrahedrally coordinated and hydrogen-bonded water, respectively.[60,61]

On the hydrophilic surface, the water structure is significantly different. After the addition of the peptide, the OH peak at $\sim$3400 cm^{-1} completely disappears in the spectrum and the intensity of the $\sim$3200 cm^{-1} peak is reduced. This suggests a significant rearrangement of the water hydrogen-bonding structure due to the peptide adsorption. The position and intensity of the OH peaks (both on the hydrophobic and hydrophilic surface) are highly dependent on the ionic strength of the buffer, the pH of the solution, and the presence of the LK_{14} peptide. The structure of water is the subject of our current investigations.

Conclusions

The combined use of the QCM-D, AFM, and SFG techniques is a powerful approach that was employed for the first time to understand and compare the in situ adsorption of a model amphiphilic peptide, LK_{14}, at the hydrophobic surface/water and hydrophilic surface/water interface. The time-dependent QCM-D and AFM studies show that LK_{14} follows a first-order monolayer adsorption over 2 min, forming a rigid film on hydrophobic PS. Alternatively, on hydrophilic SiO_2 we observe a slower multistep adsorption process leading to a more viscoelastic adsorbate with layered LK_{14} molecules, which laterally aggregate on a micrometer scale over a 30−35-min period. Multilayer formation on SiO_2 leads to a 2-fold increase in the friction, while submonolayer coverage of the peptide on PS results in minimal change in the exhibited friction. The SFG spectra indicate that the differences in morphology, friction, adsorbed amounts, and viscoelasticity, measured by QCM and AFM on the hydrophobic and hydrophobic surfaces, can be attributed to the very different nature of the molecular interaction occurring at the interface. In the LK_{14}/PS system, the SFG spectrum reveals that the adsorption is dominated by the CH interactions at the surface and suggests a predominantly hydrophobic-driven adsorption mechanism mediated by the hydrophobic side (leucine amino acid) of the peptide. Conversely, for the LK_{14}/SiO_2 system, the hydrophilic surface promotes the NH moieties to become ordered at the interface. This suggests that this surface/peptide interaction is governed by a completely different bonding mechanism. Furthermore, this surface-sensitive difference in adsorption behavior is observed on a macromolecular scale (as confirmed by AFM and QCM).

(57) Samuel, N. T.; McCrea, K. R.; Gamble, L. J.; Ward, R. S.; Stayton, P. S.; Somorjai, G. A.; Castner, D. G. Manuscript in preparation.
(58) Jung, S. Y.; Lim, S. M.; Albertorio, F.; Kim, G.; Gurau, M. C.; Yang, R. D.; Holden, M. A.; Cremer, P. S. *J. Am. Chem. Soc.* **2003**, *125*, 12782.
(59) Krimm, S.; Bandekar, J. *Adv. Protein Chem.* **1986**, *38*, 183.
(60) Du, Q.; Freysz, E.; Shen Y. R. *Science* **1994**, *264*, 826.
(61) Scatena, L. F.; Richmond G. L. *Chem. Phys. Lett.* **2004**, *383*, 491.

This combined technique approach is highly advantageous for understanding peptide behavior at the aqueous/solid interface because it independently probes the morphological and mechanical behavior, quantitative coverage amount, and molecular-scale average orientation and interaction in response to the surface hydrophobicity.

Acknowledgment. This work was supported by UC Discovery Grant BioSTAR 01-10132, and the Director, Office of Energy Research, Office of Basic Energy Sciences, Materials Science Division (LBNL), of the U.S. Department of Energy under Contract No. DE-AC02-05CH11231. We thank Prof. Carolyn Bertozzi and Jennifer Prescher (UC Berkeley) for their assistance with the peptide synthesis, and Prof. Jay T. Groves (UC Berkeley), Prof. Curtis W. Frank, and Nam-Joon Cho at the Center on Polymer Interfaces and Macromolecular Assemblies (CPIMA, Stanford University) for use of and technical help with the QCM-D instrument. Dr. Na Ji (UC Berkeley), Dr. Michael Hagan (UC Berkeley), Dr. Ralf Richter (Heidelberg University), and Patrik Björn (Q-Sense) are kindly acknowledged for helpful discussions.

JA056031H